Filtered Multitone Modulation for Very High-Speed Digital Subscriber Lines

Giovanni Cherubini, *Senior Member, IEEE*, Evangelos Eleftheriou, *Fellow, IEEE*, and Sedat Ölçer, *Senior Member, IEEE*

***Abstract*—A filter-bank modulation technique called filtered multitone (FMT) and its application to data transmission for very high-speed digital subscriber line technology are described. The proposed scheme leads to significantly lower spectral overlapping between adjacent subchannels than for known multicarrier techniques such as discrete multitone (DMT) or discrete wavelet multitone. FMT modulation mitigates interference due to echo and near-end crosstalk signals, and increases system throughput and reach. Signal equalization in an FMT receiver is accomplished in the form of per-subchannel symbol-spaced or fractionally spaced linear or decision-feedback equalization. The problem of channel coding for this type of modulation is also addressed, and an approach that allows combined removal of intersymbol-interference via precoding and trellis coding is described. Furthermore, practical design aspects regarding filter-bank realization, initial transceiver training, adaptive equalization, and timing recovery are discussed. Finally, simulation results of the performance achieved by FMT modulation for very high-speed digital subscriber line systems, where upstream and downstream signals are separated by frequency-division duplexing, are presented and compared with DMT modulation.**

***Index Terms*—Digital duplexing, filter banks, noncritical sampling, per-subchannel equalization, precoding, spectral containment, very high-speed digital subscriber line.**

I. Introduction

VERY HIGH-SPEED digital subscriber line (VDSL) is the next-generation DSL technology capable of delivering a variety of broadband services to business and residential customers. VDSL is intended to be deployed from a fiber-fed Optical Network Unit ("fiber-to-the-curb" or "fiber-to-the-cabinet" architecture), or directly from the central office premises, using the existing local-loop telephone-twisted-pair cabling for last-leg connectivity.

Reliable and cost-effective VDSL transmission at a few tens of Mb/s is made possible by the use of frequency-division duplexing (FDD), which avoids signal disturbance by near-end crosstalk (NEXT), a particularly harmful form of interference at VDSL transmission frequencies. Ideally with FDD, transmissions on neighboring pairs within a cable binder couple only through far-end crosstalk (FEXT), the level of which is significantly below that of NEXT. In practice, however, other forms of signal couplings come into play because upstream and downstream transmissions are placed spectrally as close as possible to each other in order to avoid wasting useful spectrum. Closely packed transmission bands exacerbate interband interference by echo and NEXT from similar systems (self-NEXT), possibly leading to severe performance degradation. Fortunately, it is possible to design modulation schemes that make efficient use of the available spectrum and simultaneously achieve a sufficient degree of separation between transmissions in opposite directions by relying solely on digital signal processing techniques. This form of FDD is sometimes referred to as *digital duplexing* [1], [23].

The digital duplexing method for VDSL known as Zipper [2], [3] is based on discrete-multitone (DMT) modulation. In this paper we discuss the principles of another multicarrier-modulation scheme called filtered multitone (FMT) [4], [5], a filter-bank modulation technique that involves a different set of trade-offs for achieving digital duplexing in VDSL and offers system as well as performance advantages over DMT. The specifications of transceivers based on FMT modulation have been included as an informative annex in the interim VDSL standard to be issued by ANSI [6]. We note that FMT modulation is also well-suited for wireless applications [7].

The key advantages of FMT modulation for VDSL can be summarized as follows. First, there is flexibility to adapt to a variety of spectrum plans for allocating bandwidth for upstream and downstream transmission by proper assignment of the subchannels.[1] This feature is also provided by DMT modulation, but not as easily by single-carrier modulation systems. Second, FMT modulation allows a high-level of subchannel spectral containment and thereby avoids disturbance by echo and self-NEXT. Furthermore, disturbance by a narrowband interferer, e.g., from AM or HAM radio sources, does not affect neighboring subchannels as the side lobe filter characteristics are significantly attenuated. Third, FMT modulation does not require synchronization of the transmissions at both ends of a link or at the binder level, as is sometimes needed for DMT modulation. Finally, there is no need for cyclic extensions in the form of cyclic prefix or suffix.

This paper is organized as follows. In Section II, we discuss the basic principles of FMT modulation within the context of filter-bank systems. In Section III, we describe an efficient, fast-Fourier-transform (FFT)-based transmitter and receiver implementation of filter-bank communication systems that employ "noncritical" sampling. In Section IV, we deal with the problem of per-subchannel adaptive equalization for FMT transmission characterized by spectral near-nulls at the subchannel band edges. We also address the problem of channel coding for this type of transmission and describe an approach

Manuscript received May 29, 2001; revised December 11, 2001.

The authors are with IBM Research, Zurich Research Laboratory, Säumerstrasse 4, CH-8803 Rüschlikon, Switzerland (e-mail: cbi@zurich.ibm.com; ele@zurich.ibm.com; oel@zurich.ibm.com).

Publisher Item Identifier S 0733-8716(02)05369-6.

[1]Note that, today, spectrum plans are fixed within most geographical regions.

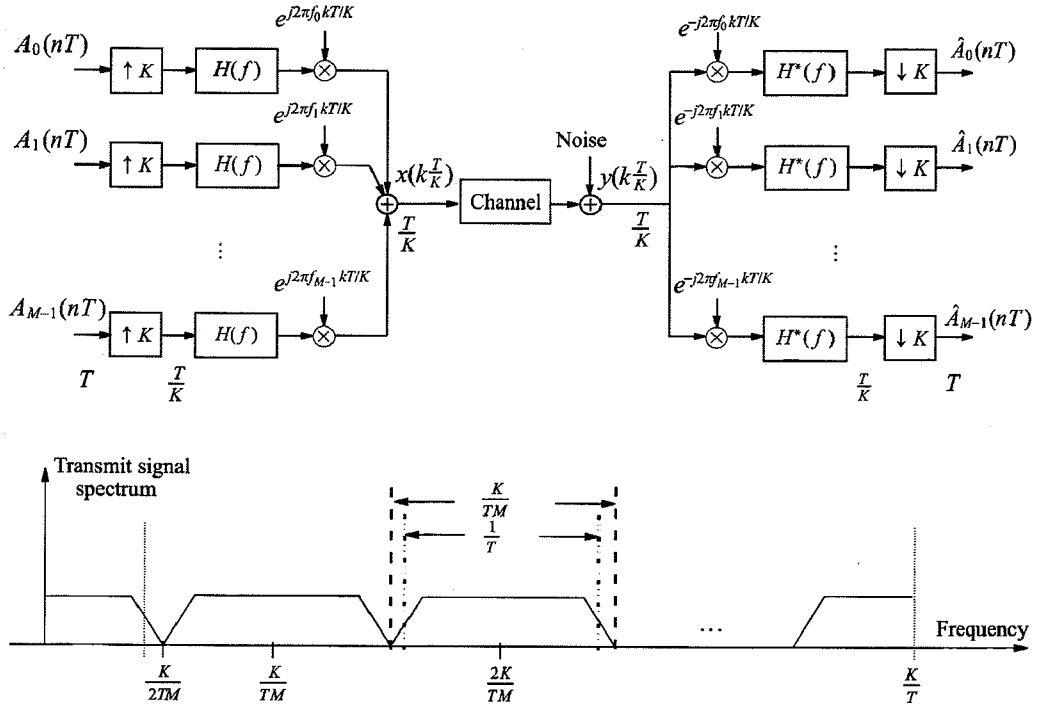

Fig. 1. Direct realization of an M-band communication system using filter-bank modulation with subchannel center frequencies $f_m = m(K/MT)$, $m = 0, \ldots, M-1$.

that allows combined removal of intersymbol-interference via precoding and trellis coding. In Section V, we consider some practical aspects of the implementation of FMT systems, including filter-bank design, adaptive equalization, symbol timing recovery and initial transceiver training. In Section VI, we give simulation results that illustrate the performance achieved by FMT modulation for VDSL transmission and also provide comparisons with DMT modulation.

II. Filter-Bank Systems and FMT Modulation

The idea of subdividing a signal frequency band into a set of contiguous bands in order to achieve efficient system realizations has pervaded the fields of signal processing and data communications for many decades. Filter banks [8] have emerged as a powerful analysis and design technique in that context.

Fig. 1 shows an M-subchannel filter-bank communication system, also referred to as a multicarrier communication system. The complex-valued modulation symbols $A_m(nT)$, $m = 0, 1, \ldots, M-1$, chosen from not necessarily identical QAM constellations, are provided at the symbol rate of $1/T$. After upsampling by a factor of K, indicated by the notation $\uparrow K$, each symbol stream is filtered by a baseband filter, referred to as a *prototype* filter, with frequency characteristic $H(e^{j2\pi f})$ and impulse response $h(k)$. The transmit signal $x(kT/K)$ is obtained at the transmission rate of K/T by adding the M filter-output signals properly shifted in frequency. At the receiver, matched filtering (whereby $*$ denotes complex conjugation) is employed, followed by subsampling by a factor of K indicated by the notation $\downarrow K$. When $K = M$ ($K > M$), the filter bank is said to be *critically* (*noncritically*) sampled. Fig. 1 also illustrates the way in which the parameters K, M, and $1/T$ determine the spectral characteristic of the transmitted signal.

The inherent signal shaping capability of filter-bank systems offers several degrees of freedom to the communication system designer. Traditionally, filter characteristics have been chosen to satisfy a "perfect reconstruction" constraint in order to ensure that transmission is free of intersymbol interference (ISI) within a subchannel as well as free of interchannel interference (ICI). Assuming critical sampling at the transmitter, transmission over an ideal channel and matched filtering at the receiver, the "perfect reconstruction" conditions are expressed in the time domain as [8]

$$\sum_k h_i(k) h_{i'}^*(k - lM) = \delta_{i-i'}\delta_l,$$
$$0 \le i, i' \le M-1, \quad l = \ldots, -1, 0, 1, \ldots \qquad (1)$$

where $h_i(k) = h(k)e^{j2\pi ki/M}$ and δ_i is the Kronecker delta. The elements of a set of orthogonal filter impulse responses that satisfy (1), which can be interpreted as a more general form of the Nyquist criterion, are sometimes referred to as *wavelets*.

For example, the perfect reconstruction conditions are satisfied in the case of DMT systems, for which $K = M$ and the impulse response of the prototype filter is selected as

$$h(k) = \begin{cases} 1, & \text{for } 0 \le k \le M-1 \\ 0, & \text{otherwise} \end{cases} \quad \Leftrightarrow$$
$$H(e^{j2\pi f}) = \frac{\sin(\pi f M)}{\sin(\pi f)} e^{-j(M-1)\pi f}. \qquad (2)$$

Fig. 2(a) shows the spectral subchannel characteristics obtained with DMT for $M = 64$. We see that the spectra of adjacent subchannels approximately cross at the -3-dB point and that the first sidelobe is as high as -13 dB. Discrete wavelet multitone (DWMT) [9] modulation is another example of a multicarrier modulation scheme for which the perfect reconstruction conditions hold. In that case, although the sidelobes are fairly attenuated, the spectra of adjacent subchannels still cross at -3 dB,

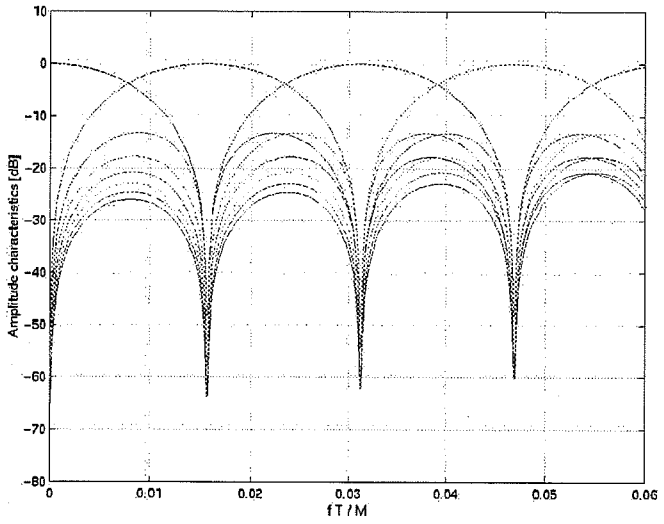

(a)

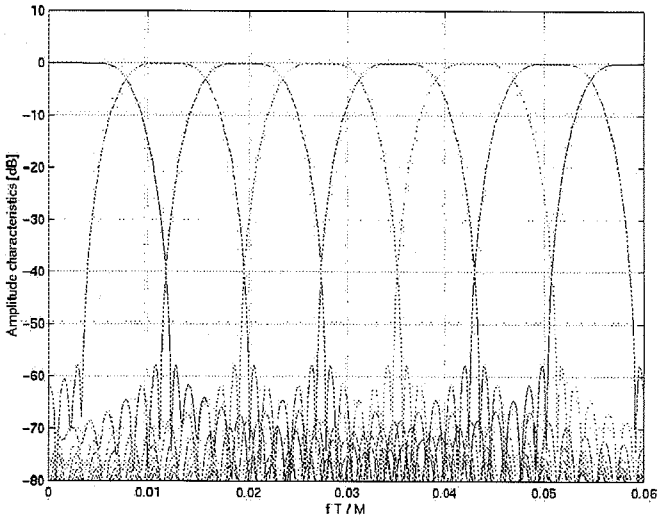

(b)

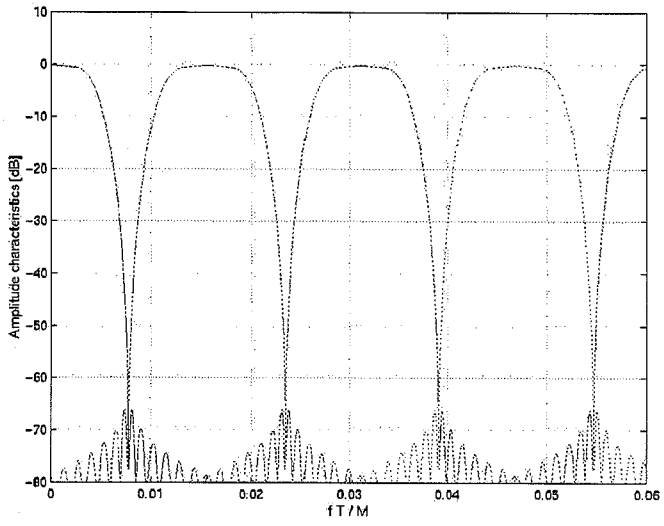

(c)

Fig. 2. Subchannel frequency responses for $f \in [0, 0.06M/T]$ and $M = 64$. (a) DMT. (b) DWMT. (c) FMT.

see Fig. 2(b). In DWMT modulation, all signal processing operations involve real signals and, for an M-subchannel transmit signal, each subchannel occupies half the bandwidth of a subchannel for DMT or FMT modulation. We note that perfect reconstruction usually requires that substantial overlap of adjacent subchannels be allowed.

It is generally not practical to include the characteristics of the nonideal transmission channel in the perfect reconstruction conditions. Consequently, the orthogonality between subchannels is destroyed at the receiver whenever amplitude and phase distortion are introduced by the transmission medium, causing in most cases unacceptable performance degradation. To maintain orthogonality, DMT modulation systems extend cyclically each block of M transmit symbols prior to transmission. The FMT modulation technique described in this paper follows another approach, whereby spectral overlap between the subchannels is avoided by resorting to noncritically sampled filter-bank systems and employing per-branch filter characteristics that achieve tight subchannel spectral containment. Fig. 2(c) shows the spectral characteristics of consecutive subchannels that are obtained for an FMT system with $M = 64$ and per-subchannel finite-impulse response (FIR) filters with ten coefficients. Note that the spectral energy outside of a subchannel is suppressed by more than 67 dB, with further suppression possible by increasing the length of the prototype filter.

Clearly, achieving orthogonality either in the form of nonoverlapping subchannel characteristics or through the use of cyclic extensions involves a penalty in terms of spectral efficiency. If this penalty is comparable for both approaches, then the former is preferred in the case that unique benefits are derived from a high level of spectral containment. This property is, for example, attractive for wired network access, where the unbundling of the local loop and the mixture of asymmetric and symmetric transmissions over the same cable raise the sensitivity to potential crosstalk generated by the overlap of adjacent frequency bands of different services. In other words, tight subchannel spectral containment is good for spectrum management.

To summarize, FMT represents a filter-bank modulation technique where the M-branch filters are frequency-shifted versions of a prototype filter that achieves a high level of spectral containment, such that the ICI is negligible compared to other noise signals. High spectral containment is more easily achieved by relaxing the perfect reconstruction constraint and by resorting to noncritically sampled filter banks. In Section III, we derive an equivalent efficient realization for the noncritically sampled filter bank structure shown in Fig. 1.

III. Efficient Realization of FMT Modulation

At time kt/K, the signal $x(kT/K)$ input to the channel is given by (see Fig. 1)

$$\begin{aligned} x\left(k\frac{T}{K}\right) &= \sum_{m=0}^{M-1}\sum_{n=-\infty}^{+\infty} A_m(nT)h\left[(k-nK)\frac{T}{K}\right] \\ &\quad \times e^{j2\pi m(K/MT)k(T/K)} \\ &= \sum_{n=-\infty}^{+\infty}\sum_{m=0}^{M-1} A_m(nT) \\ &\quad \times e^{j2\pi m(K/MT)k(T/K)}h\left[k\frac{T}{K}-nT\right]. \end{aligned} \tag{3}$$

With the change of variables $kT/K = (lM + i)(T/K)$, $i = 0, 1, \ldots M-1$, we get

$$x\left(lM\frac{T}{K}+i\frac{T}{K}\right)=\sum_{n=-\infty}^{+\infty}\sum_{m=0}^{M-1}A_m(nT) \times e^{j2\pi m(K/MT)i(T/K)}h\left(lM\frac{T}{K}+i\frac{T}{K}-nT\right). \quad (4)$$

By introducing $a_i(nT) \triangleq \sum_{m=0}^{M-1} A_m(nT)e^{j2\pi(mi/M)}$, we can write (4) as

$$x\left(lM\frac{T}{K}+i\frac{T}{K}\right)=\sum_{n=-\infty}^{+\infty}a_i(nT)h\left(lM\frac{T}{K}+i\frac{T}{K}-nT\right). \quad (5)$$

Clearly, $a_i(nT), i = 0, \ldots, M-1$ are obtained from $A_m(nT)$, $m = 0, \ldots, M-1$ via an inverse discrete Fourier transform (IDFT). Furthermore, by adopting the general expression for signal interpolation where a "filter index" $q = \lfloor (lM+i)/K \rfloor - n$, a "basepoint index" $\eta_{l,i} = \lfloor (lM+i)/K \rfloor$, and a "fractional index" $\nu_{l,i} = \lfloor (lM+i)/K \rfloor - \eta_{l,i}$ are introduced [10], we can express the transmit signal as

$$\begin{aligned}x\left(lM\frac{T}{K}+i\frac{T}{K}\right)&=\sum_{q=-\infty}^{+\infty}a_i[(\eta_{l,i}-q)T]\,h[(\nu_{l,i}+q)T]\\&=\sum_{q=-\infty}^{+\infty}a_i[(\eta_{l,i}-q)T]\,h^{(\nu_{l,i}K)}(qT)\\&\qquad i=0,1,\ldots,M-1 \quad (6)\end{aligned}$$

where $0 \le \nu_{l,i} < 1$ and $\nu_{l,i}K = (lM+i) \bmod K$. Hence, we find that the transmit signal at time kT/K is computed by convolving the signal samples stored in the $(k \bmod M)$th delay line at the IDFT output with the $(k \bmod K)$th polyphase component (with respect to K) of the prototype filter. In other words, the integer number $\nu_{l,i}K$ provides the address of the polyphase component that needs to be applied at the $(k \bmod M)$th output of the IDFT to generate the transmitted signal $x(kT/K)$. Therefore, each element of the IDFT output frame is filtered by a periodically time-varying filter with period equal to $[\mathrm{lcm}(M, K)]T/K$, where $[\mathrm{lcm}(M, K)]$ denotes the least common multiple of M and K. This transmitter structure is depicted in Fig. 3.

Note that the mth subchannel, $m = 0, \ldots, M-1$, can be considered a prototype baseband channel that is translated in frequency by $f_m = m(K/MT)$ Hz, as shown in Fig. 1. By resorting to noncritically sampled filter banks, modulation with an excess bandwidth of $\alpha = K/M - 1$ within each subchannel is feasible and ensures total spectral containment within a subchannel. By letting $K \to M$, the penalty in bandwidth efficiency becomes vanishingly small at the price of an increase in implementation complexity because filters with increasingly sharper spectral roll-off must then be realized.

For a critically sampled system with $K = M$, the efficient realization shown in Fig. 3 becomes equivalent to that obtained in [11]. In that case each element of the IDFT output frame is processed by a filter that is no longer periodically time varying.

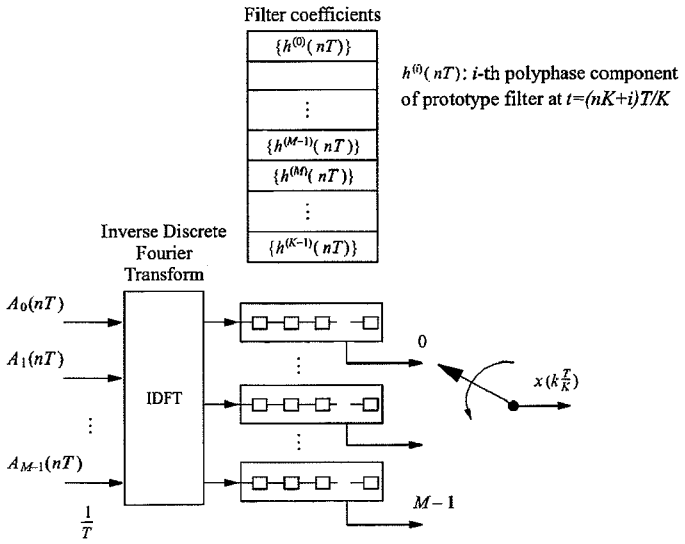

Fig. 3. Efficient implementation of the FMT modulator.

We now turn to the efficient implementation of the FMT demodulator, where we assume for the received signals the same sampling rate as for the transmit signals and consider in general a subsampling factor $L \le K$ (i.e., in Fig. 1, replace $\downarrow K$ with $\downarrow L$). The received signal is, thus, denoted by $y(kT/K)$ and the filtering elements on the M branches are given by polyphase components (with respect to M) of a prototype filter $\{g(kT/K)\}$ with T/K-spaced coefficients, defined as $\{g^{(m)}(l(MT/K))\} = \{g[(lM+m)(T/K)]\}$, $m = 0, 1, \ldots, M-1$.

The ith output signal of the FMT demodulator at time $n'(L/K)T$ is given by

$$z_i\left(n'\frac{L}{K}T\right)=\sum_{k=-\infty}^{+\infty}y\left(k\frac{T}{K}\right) \times e^{-j2\pi i(K/MT)k(T/K)}\,g\left[(Ln'-k)\frac{T}{K}\right]. \quad (7)$$

Letting $k(T/K) = (lM+m)(T/K)$, $m = 0, 1, \ldots M-1$, we obtain

$$z_i\left(n'\frac{L}{K}T\right)=\sum_{m=0}^{M-1}\sum_{l=-\infty}^{+\infty}y\left[(lM+m)\frac{T}{K}\right] \times g\left[(Ln'-lM-m)\frac{T}{K}\right]e^{-j2\pi(im/M)} \quad (8)$$

which can be expressed as

$$z_i\left(n'\frac{L}{K}T\right)=\sum_{m=0}^{M-1}u_m\left(n'\frac{L}{K}T\right)e^{-j2\pi(im/M)} \quad (9)$$

where

$$u_m\left(n'\frac{L}{K}T\right)\triangleq\sum_{l=-\infty}^{+\infty}y\left[(lM+m)\frac{T}{K}\right] \times g\left[(Ln'-lM-m)\frac{T}{K}\right]. \quad (10)$$

Clearly, $z_i(n'(L/K)T)$, $i = 0, \ldots, M-1$, are obtained from $u_m(n'(L/K)T)$, $m = 0, \ldots, M-1$, via a discrete Fourier transform (DFT). Furthermore, if we define the polyphase

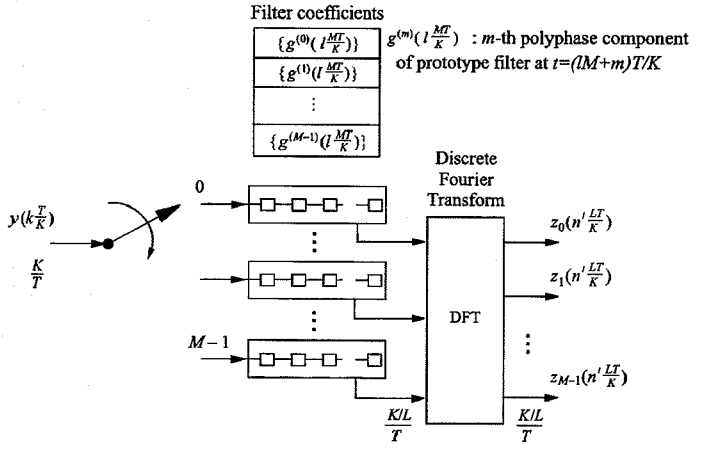

Fig. 4. Efficient implementation of the FMT demodulator.

components (with respect to M) of the received signal as $y^{(m)}(l(MT/K)) = y[(lM+m)(T/K)], m = 0, \ldots, M-1$, and introduce a "filter index" $q' = \lfloor (Ln' - m)/M \rfloor - l$, a "basepoint index" $\eta'_{n',m} = \lfloor (Ln' - m)/M \rfloor$, and a "fractional index" $\nu'_{n',m} = \lfloor (Ln' - m)/M \rfloor - \eta'_{n',m}$, we obtain

$$u_m\left(n'\frac{L}{K}T\right) \triangleq \sum_{q'=-\infty}^{+\infty} y^{(m)}\left[(\eta'_{n',m} - q')\frac{MT}{K}\right] \times g^{(\nu'_{n',m}M)}\left(q'\frac{MT}{K}\right). \quad (11)$$

Note that if the receive prototype filter is causal and matched to the transmit prototype filter, i.e., $\{g(kT/K)\} = \{h^*(\gamma M - kT/K)\}$, where γM denotes the filter length assumed to be a multiple of M, then (11) becomes

$$u_m\left(n'\frac{L}{K}T\right) \triangleq \sum_{l=-\infty}^{+\infty} y\left[\left(l+\frac{m}{M}\right)\frac{MT}{K}\right] \times \left\{h\left[\left(l+\gamma+\frac{m-Ln'}{M}\right)\frac{MT}{K}\right]\right\}^*. \quad (12)$$

In general, a new DFT output frame at time $kT/K = n'LT/K$ is obtained by the following method (see Fig. 4): the commutator is circularly rotated L steps from its position at time $(n'-1)/T$, allowing a set of L consecutive received signals $y(kT/K)$ to be input into the M delay lines. The content of each delay line is then convolved with a polyphase component (with respect to M) of the receive prototype filter. The integer number $\nu'_{n',m}M$ provides the address of the polyphase component that needs to be applied at the mth branch. The resulting signals are then input to the DFT to finally yield the signals $z_i(n'(L/K)T), i = 0, \ldots, M-1$. Note that the DFT output frames are obtained at the rate of $(K/L)/T$.

Clearly, it is possible to consider in general an FMT system where the sampling rate of the analog-to-digital (A/D) converter is given by K'/T, with $K' > K$. In this case a digital interpolation filter is first employed to convert the rate of the received signal samples from K'/T to K/T. The obtained signal is then input to the FMT demodulator.

IV. Per-Subchannel Adaptive Equalization and Precoding

We recall that the frequency responses of FMT subchannels are characterized by steep roll-off toward the band-edge frequencies, where they exhibit near spectral nulls. This suggests that per-subchannel decision-feedback equalization be performed to recover the transmitted symbols. In this section, we address this topic and also consider the application of precoding techniques to FMT modulation. Note that per-subchannel equalization has also been recently proposed for DMT-based systems [12].

The block diagram of an FMT receiver employing per-subchannel equalization is illustrated in Fig. 5. The signals $z_i(n'(LT/K)), i = 0, \ldots, M-1$, at the FMT demodulator output are input for symbol detection to M adaptive decision-feedback equalizers having feed-forward linear sections with $L'T/K$-spaced coefficients, where L'/L is an integer number. If we define the coefficient vectors of the feedforward linear section and of the feedback section of the ith equalizer at time nT as $\mathbf{c}_i(nT) = \mathbf{c}_{i,n} = \{c^{(i)}_{l,n}, l = 0, \ldots, N_f - 1\}$ and $\mathbf{q}_i(nT) = \mathbf{q}_{i,n} = \{q^{(i)}_{l,n}, l = 1, \ldots, N_b\}$, respectively, the equalizer output on the ith subchannel at time nT is given by

$$d_i(nT) = \sum_{l=0}^{N_f-1} z_i\left[\left(n\frac{K}{L} - l\frac{L'}{L}\right)\frac{LT}{K}\right] c^{(i)}_{l,n} - \sum_{l=1}^{N_b} \times \hat{A}_i[(n-l)T] q^{(i)}_{l,n} \quad (13)$$

where K/L is also assumed to be an integer and $\hat{A}_i(nT)$ denotes the symbol decision on the ith subchannel at time nT, which is provided by a memoryless decision element. Note that the choice $L = L' = K/2$ results in fractionally $T/2$-spaced coefficients of the linear feedforward equalizer section.

Error propagation inherent to decision-feedback equalization can be avoided by resorting to precoding techniques. For example, per-subchannel Tomlinson–Harashima precoding [13] can be applied in a straightforward manner and was assumed in Fig. 5, where only the linear forward equalizers are shown at the receiver. The application of precoding techniques in conjunction with trellis-coded modulation (TCM) for FMT transmission requires further discussion.

Flexible precoding [13] or *trellis-enhanced precoding* [14] for trellis-coded transmission over an ISI channel allows coding gains to be achieved for arbitrary constellations provided that the ISI channel is linearly invertible. However, if the channel exhibits spectral nulls, as is usually the case for an FMT subchannel characteristic, infinite error propagation can occur within the inverse precoder at the receiver. In that case, feedback trellis encoding can still be achieved by *trellis-augmented precoding* [15], but only certain constellations are then allowed. With trellis-augmented precoding, error propagation in the FMT receiver is completely avoided.

Trellis-augmented precoding for FMT transmission is described in detail in Appendix A. For transmission over the mth subchannel, an $N_m \times N_m$-point signal constellation is assumed, with N_m even, $\forall m$. The transmitter consists of

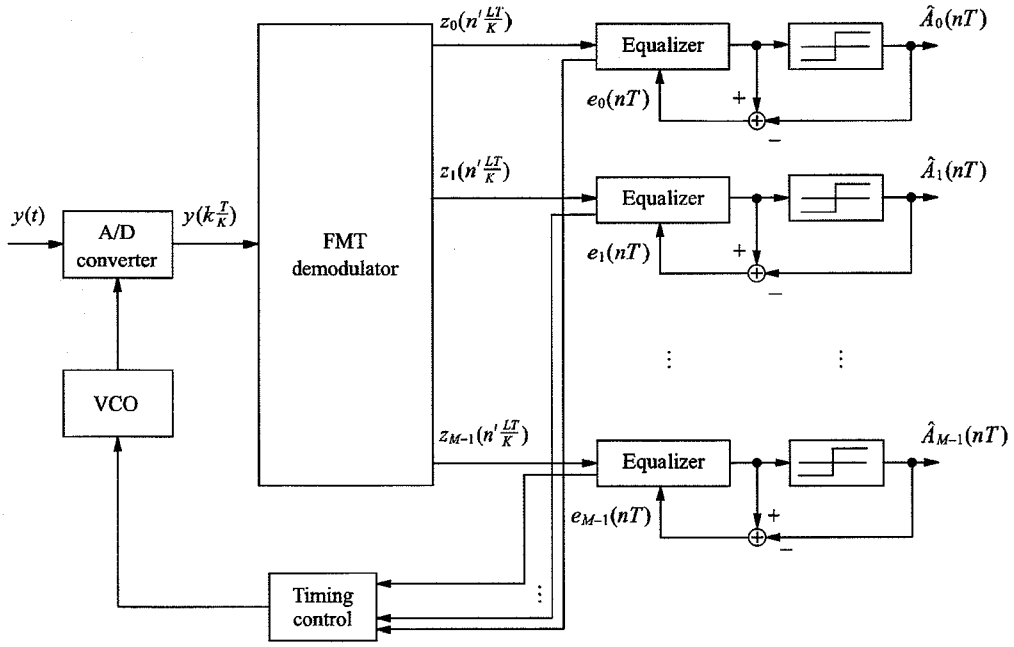

Fig. 5. Block diagram of an FMT receiver with per-subchannel equalization.

M units chained together to allow trellis coding across the subchannels. This arrangement is chosen to reduce decoding delay and is possible because transmission over M independent subchannels may be assumed.

V. Practical Considerations

A. Filter-Bank Design

Filter-bank design for FMT modulation is discussed in Appendix B. In this approach a linear phase FIR prototype filter of length γM is determined that approximates a filter with suitable frequency response characteristic $H_{\text{ideal}}(e^{j2\pi fT})$. Then each of the polyphase filter components (with respect to M) has γ coefficients. The parameter γ is defined as the *overlap factor* of the system.

The first example of prototype filter design for FMT systems we consider is the target frequency response given by

$$H_{\text{ideal},1}(e^{j2\pi fT}) = \begin{cases} \left|\dfrac{1+e^{-j2\pi fT}}{1+\varrho e^{-j2\pi fT}}\right|, & \text{if } -1/2T \le f \le 1/2T \\ 0, & \text{otherwise,} \end{cases} \tag{14}$$

where the parameter $0 \le \varrho \le 1$ controls the spectral "roll-off" of the filter. The frequency response $H_{\text{ideal},1}(e^{j2\pi fT})$ exhibits spectral nulls at the band edges and, when used as the prototype filter characteristic, leads to transmission free of ICI but with ISI within a subchannel. For $\varrho \to 1$, the frequency characteristic of each subchannel is characterized by steep roll-off toward the band edge frequencies. On the other hand for $\varrho = 0$ one obtains the partial-response class I characteristic. Fig. 2(c) shows the spectral characteristics of consecutive subchannels that are obtained by using a prototype FIR filter designed for M =64, $\varrho = 0.1$, and $\gamma = 10$. For transmission with 0%, 6.25%, or 12.5% excess bandwidth within a subchannel, a modulator with upsampling parameter values of $K = 64$, $K = 68$, or $K = 72$ would be chosen, respectively.

Another choice for the target filter characteristic is obtained if the prototype filter design is based on a square-root raised cosine Nyquist filter with excess bandwidth α, i.e.,

$$H_{\text{ideal},2}(e^{j2\pi fT}) = \begin{cases} 1, & \text{if } |f| \le (1-\alpha)/2T \\ \dfrac{1}{\sqrt{2}}\sqrt{1-\sin\dfrac{\pi}{\alpha}\left(fT-\dfrac{1}{2}\right)}, & \text{if } (1-\alpha)/2T \\ & \le |f| \le (1+\alpha)/2T \\ 0, & \text{otherwise.} \end{cases} \tag{15}$$

The frequency response $H_{\text{ideal},2}(e^{j2\pi fT})$ leads to transmission free of ICI and ISI within a subchannel if the channel is ideal. In other words, the perfect reconstruction conditions are, in this case, satisfied.

B. Adaptive Equalization and Timing Recovery

In a practical system employing decision-feedback equalization at the receiver the adjustment of the equalizer coefficients can be achieved by using the standard least mean square (LMS) algorithm

$$\mathbf{c}_{i,n+1} = \mathbf{c}_{i,n} - \mu e_{i,n}\mathbf{z}^*_{i,n} \tag{16}$$

$$\mathbf{q}_{i,n+1} = \mathbf{q}_{i,n} - \mu e_{i,n}\hat{\mathbf{A}}^*_{i,n} \tag{17}$$

where $\mu > 0$ is a suitably selected adaptation gain, $e_{i,n} = e_i(nT) = d_i(nT) - \hat{A}_i(nT)$, $\mathbf{z}_{i,n} = \{z_i[(n(K/L) - l(L'/L))(LT/K)], l = 0, \ldots, N_f - 1\}$, and $\hat{\mathbf{A}}_{i,n} = \{\hat{A}_i[(n-l)T], l = 1, \ldots N_b\}$. If the feedback filter is implemented as a precoder, then after the adaptation procedure is over the coefficients are sent to the transmitter during the transceiver initialization protocol. Furthermore, the mean-square errors that are used for training the per-subchannel equalizers can be used to provide estimates of the signal-to-noise ratios (SNRs) at the M equalizer decision points, defined as

$\mathrm{SNR}_i = E[|\hat{A}_i(nT)|^2]/E[|e_i(nT)|^2]$, $i = 0, \ldots, M-1$. These values are continuously monitored and used to assist in various receiver functions during initialization as well as during data mode.

The sampling phase of the A/D converter is determined by a clock generated by a voltage-controlled oscillator (VCO). The control signal to the VCO is provided by a timing control unit, which receives M digital input signals $\Delta\tau_{i,n}$, $i = 0, \ldots, M-1$, from the M subchannel outputs, as illustrated in Fig. 5. These input signals may be computed by a decision-directed timing recovery algorithm [16], given by

$$\Delta\tau_{i,n} = \mathrm{Re}[d_i(nT) - d_i((n-2)T)] \times\{\mathrm{Re}[e_i((n-1)T)] - \mathrm{Im}[e_i((n-1)T)]\}. \quad (18)$$

A straightforward strategy for the timing control unit is to select the signal that is received from the output of the subchannel where the largest SNR is observed. Say this is the subchannel with index $\hat{\imath}$. The selected signal $\Delta\tau_{\hat{\imath},n}$ is then input to a second-order loop filter. The filter output $\Delta\tau_{s,n}$ and the value $u_{\mathrm{acc},n}$ that is stored in the accumulator of the loop filter are given by

$$\Delta\tau_{s,n} = \gamma_s \Delta\tau_{\hat{\imath},n} + u_{\mathrm{acc},n} \quad (19)$$

and

$$u_{\mathrm{acc},n+1} = u_{\mathrm{acc},n} + \zeta_s \Delta\tau_{\hat{\imath},n} \quad (20)$$

where γ_s and ζ_s are suitably selected loop gains. The filter output $\Delta\tau_{\hat{\imath},n}$ is then converted into an analog signal, which is input to the VCO.

C. Echo Cancellation

For applications that require full-duplex transmission over the entire band, echo cancellation for full-duplex FMT systems can be performed entirely in the frequency domain by taking into account for each subchannel only the echo generated by transmission in the opposite direction on the same subchannel. Per-subchannel echo cancellation then requires in general M adaptive echo cancelers. Note that if the attenuation of echo signals from adjacent subchannels is not sufficient, echo cancellation can still be achieved by using $2M$ additional adaptive periodically time-varying echo cancelers.

D. Training Procedure for VDSL

In principle, for the initialization of an FMT-based VDSL transceiver, the same set of transmit sequences can be used as those specified for ADSL [17], after proper adjustments to fit VDSL specific framing and transmission constraints. These sequences allow acquisition of gain and symbol timing and permit channel identification, based on which initial equalizer coefficients and bit loading algorithms can be computed. Such an approach was shown to be effective for transmission in typical VDSL noise environment [18], [24].

VI. Numerical Results

In this section, simulation results are presented to illustrate the performance achieved by FMT-based FDD systems for VDSL and compare with that of DMT-based FDD systems.

In general, signal attenuation in decibel and phase distortion in radians introduced by homogeneous metallic transmission lines increase proportionally to the cable length and the square root of frequency due to the skin effect. We assume the following channel frequency response, which corresponds to voice-grade unshielded twisted-pair cables (UTP-3) characteristics [19]:

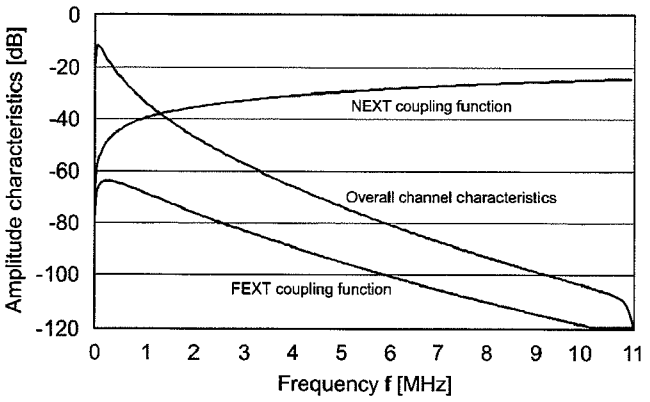

Fig. 6. Average NEXT and FEXT coupling functions and overall channel characteristic for sampling rate of 22.08 Msample/s and cable length of 1 km.

$$G_{CA}(f, l) = e^{-3.85\times10^{-6}(1+j)\sqrt{f}l} \quad (21)$$

where the constant propagation delay has been ignored. Deviations from the ideal $\sqrt{f}$ characteristic may be caused by dielectric insulation losses, connectors, presence of bridged taps, and nonhomogeneous transmission lines.

For the results presented in this section, the power spectral densities of NEXT and FEXT signals arising from disturbers, all having the same power spectral density $\mathrm{PSD}(f)$, are modeled as

$$\mathrm{PSD}_{\mathrm{NEXT}}(f) = \mathrm{PSD}(f)\left(\frac{N}{49}\right)^{0.6} 10^{-13} f^{3/2} \quad (22)$$

and

$$\mathrm{PSD}_{\mathrm{FEXT}}(f) = \mathrm{PSD}(f)|G_{CA}(f, l)|^2 \left(\frac{N}{49}\right)^{0.6} \times (3\times10^{-19}) l f^2 \quad (23)$$

respectively. Fig. 6 shows the average NEXT coupling function, which exhibits the familiar increase of 15 dB/decade, the average FEXT coupling function, and the amplitude characteristic of the overall channel transfer function for a cable length of $l = 1$ km.

Performance is measured in terms of achievable bit rate for given channel characteristics. The number of bits per modulation interval that can be loaded on the ith subchannel is given by [20]

$$\beta_i = \begin{cases} \frac{1}{2}\log_2\left(1 + \frac{\mathrm{SNR}_i\gamma_{\mathrm{code}}}{\Gamma\gamma_{\mathrm{margin}}}\right), & \text{if } i = 0 \text{ or } M/2 \\ \log_2\left(1 + \frac{\mathrm{SNR}_i\gamma_{\mathrm{code}}}{\Gamma\gamma_{\mathrm{margin}}}\right), & \text{otherwise} \end{cases} \quad (24)$$

where SNR_i is the SNR at the ith subchannel output, γ_{code} is the coding gain, Γ denotes the "SNR gap" between the minimum SNR required for reliable transmission of β bits per modulation interval and the SNR required by 2^β-ary QAM modulation to achieve a bit-error probability of 10^{-7}, $\beta \gg 1$, and γ_{margin} denotes the required additional margin [20, p. 155]. The achievable bit rate for downstream or upstream transmission is, therefore,

obtained by summing the values given by (24) over the subchannels allocated for downstream or upstream transmission and by multiplying the result by the modulation rate, and is given by

$$R = \frac{1}{T} \sum_{i=0}^{M/2} \beta_i \quad [\text{b/s}]. \tag{25}$$

The FMT systems considered here employ the same linear-phase prototype filters for the realization of transmit and receive polyphase filter banks. The prototype filters are designed for overlap factors that are in the range from 10 to 20, see Appendix B. For given number of subchannels M, the parameter K is selected to achieve a desired excess bandwidth of $\alpha = K/M - 1$. Achievable bit rates are computed for symmetric transmission with a sampling rate of 22.08 Msample/s, a transmit signal power of 10 dBm, an additive white Gaussian noise (AWGN) power spectral density equal to -140 dBm/Hz, and an echo signal that is negligible compared to the other disturbances. Per-subchannel equalization is performed by employing a Tomlinson–Harashima precoder [13] with N_b taps and a $T/2$-spaced linear equalizer with N_f taps. In the case of zero excess-bandwidth modulation, the coefficients of the linear equalizer are T-spaced. The coefficients of the linear equalizer and of the precoder are equivalent to the coefficients of the forward section and of the feedback section of a minimum mean-square-error decision-feedback equalizer (DFE), respectively, and are computed assuming perfect knowledge of the subchannel characteristics.

For comparison, the rates achieved by a synchronous DMT-based Zipper system with $M = 4096$ subchannels, cyclic prefix of 150 samples, cyclic suffix of 175 samples, no time-domain equalizer and one-tap frequency equalizers have also been determined. Perfect knowledge of the overall channel characteristics has been assumed, as well as perfect synchronization of all transmissions over the 50-pair cable. Hence, the DMT system considered here achieves ideal suppression of NEXT interference. The results are presented in Figs. 7 and 8 for an FMT system with $M = 256$ subchannels, and a prototype filter designed for $\gamma = 10$. Fig. 7 indicates that FMT and DMT-based zipper systems exhibit essentially identical performance for cable lengths up to ~700 m. For longer cables, where cable-dependent signal distortion becomes more significant, the FMT system allows higher data rates to be achieved due to its more powerful equalization capability. Fig. 8 shows various tradeoffs in terms of excess bandwidth α and number of filter coefficients N_f and N_b for linear equalization and Tomlinson–Harashima precoding, respectively. Note that in all cases the FMT-based scheme requires no synchronization of transmissions.

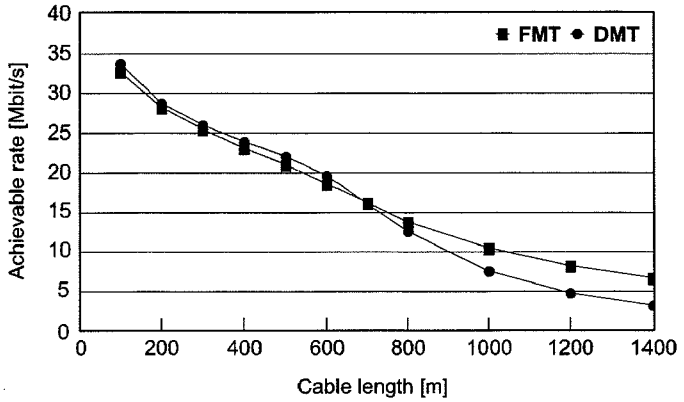

Fig. 7. Performance of FMT ($M = 256$) and synchronous DMT ($M = 4096$) for symmetric transmission. For FMT modulation, an excess bandwidth of $\alpha = 0.125$ is assumed and the number of filter coefficients for linear equalization and Tomlinson–Harashima precoding are chosen as $N_f = 36$ ($T/2$ spaced) and $N_b = 12$, respectively.

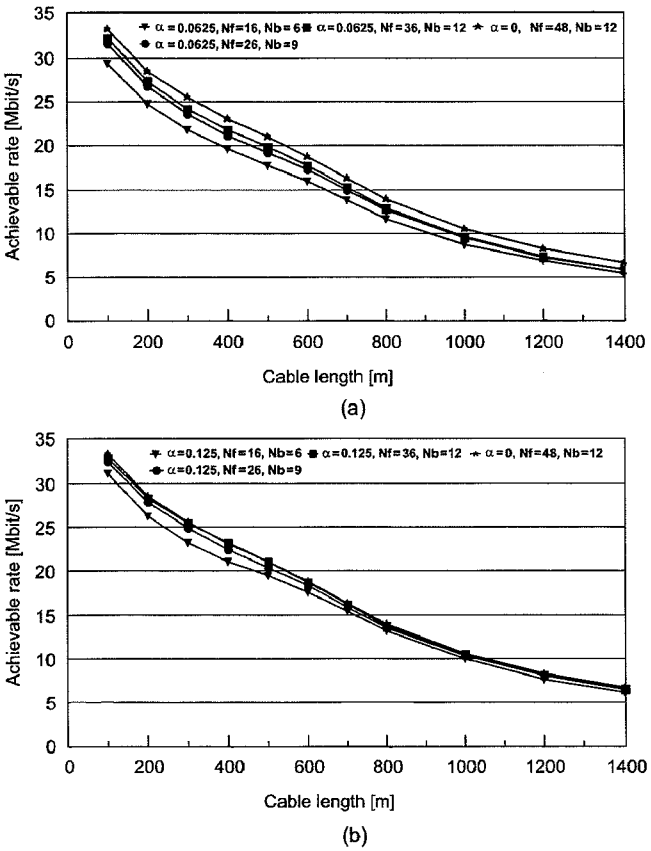

Fig. 8. Performance of FMT systems for symmetric transmission with $M = 256$ subchannels. (a) Excess bandwidth $\alpha = 0.0625$. (b) Excess bandwidth $\alpha = 0.125$. Performance with zero excess bandwidth is also indicated. N_f and N_b denote the number of filter coefficients for linear equalization and Tomlinson–Harashima precoding, respectively.

VII. Conclusion

FMT modulation is an interesting solution for VDSL transmission, being intermediate to other proposed single carrier and multicarrier methods, as well as providing some unusual advantages in terms of spectrum management, unbundling, and duplexing. FMT generates digitally a set of tightly packed single-carrier-like multiband signals with minimum analog filtering requirements and offers filtering-based implementation alternatives to the time-domain prefixing and suffixing that characterize DMT implementations. Hence, digital duplexing is achieved in FMT by filtering rather than through the use of a cyclic suffix and the consequent loop-timing of frames.

An FDD scheme based on FMT modulation exhibits robustness against various interferences such as self-NEXT, echo, and narrowband radio signals, and does not require synchronization between transmissions taking place over the same multipair cable, thus, also allowing simpler system operations.

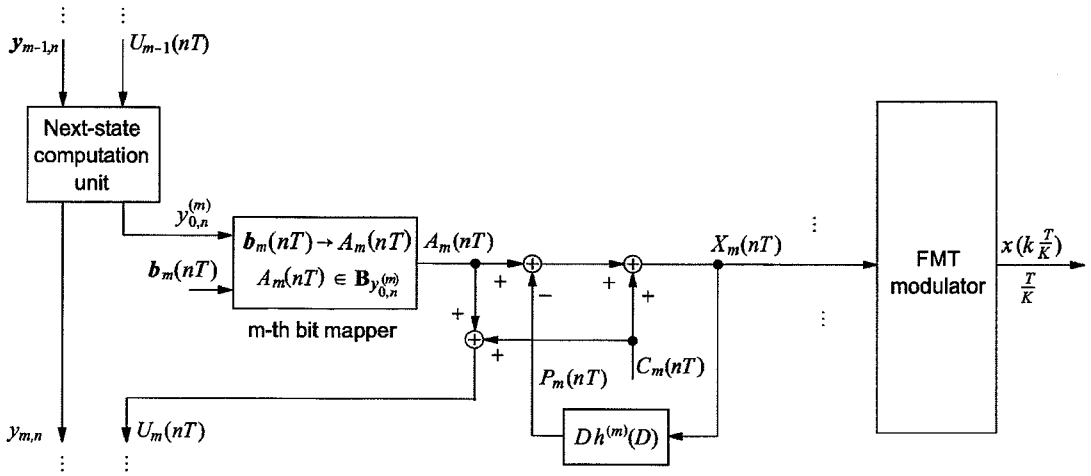

Fig. 9. FMT transmitter with trellis-augmented precoding.

Comparedf to a DMT-based scheme, enhanced performance is obtained at the cost of per-subchannel filtering, which however corresponds to functions performed at a significantly lower rate than the transmission rate.

The FMT technique described here can be extended in various ways by using the framework of filter bank systems. It can be applied to a number of difficult transmission environments, not limited to VDSL, but possibly including home local area networks (LANs), corporate LANs, cable modems and possibly even wireless transmission, in which case other equalization techniques than the ones described in this paper may be needed.

APPENDIX A
TRELLIS-AUGMENTED PRECODING FOR FMT

The block diagram of an FMT transmitter that employs trellis-augmented precoding is illustrated in Fig. 9. The mth subchannel frequency response is denoted by $h_m(D) = 1 + h^{(m)}(D) = 1 + h_1^{(m)}D + h_2^{(m)}D^2 + \cdots$. We consider a trellis code with 2^ν states and conventional encoding based on a systematic convolutional encoder. For transmission over the ith subchannel, we employ a $N_m \times N_m$-point signal constellation, with N_m even, $\forall\, m$.

For the remaining part of this appendix, we assume that the reader is familiar with precoding techniques, such as those described in [13] and [14].

To explain transmitter operations, we assume that the subchannels with indices from 1 to $M/2 - 1$ are used for transmission. Let us consider the mth trellis precoding element. At the nth modulation interval, the inputs to this element are the binary information vector $\mathbf{b}_m(nT)$, which may take one of $N_i^2/2$ different values, and the binary value $y_{0,n}^{(m)}$, which represents the least-significant bit of the TCM state $\mathbf{y}_{m,n} = (y_{\nu-1,n}^{(m)}, \cdots, y_{0,n}^{(m)})$ at the ith subchannel during the nMth modulation interval. The mapping of information bits into symbols operated by the ith signal mapper follows the usual rules of trellis coding. In particular, we note that $A_m(nT) \in \mathbf{B}_{y_{0,n}^{(m)}}$, $y_{0,n}^{(m)} \in \{0, 1\}$, where $\mathbf{B}_0$ and $\mathbf{B}_1$ are the two sets obtained at the first partitioning level of the $N_m \times N_m$-point signal constellation of the mth subchannel.

The ith precoder operates on the symbol $A_m(nT)$ and determines the mth subchannel input signal $X_m(nT)$. The sequence of the mth subchannel input signals is given by

$$X_m(D) = A_m(D) + C(D) - P_m(D) \tag{26}$$

where

$$P_m(D) = [h_m(D) - 1]X_m(D) = Dh^{(m)}(D)X_m(D) \tag{27}$$

and

$$C_m(D) = -Q_{\Lambda_X^{(m)}}\{A_m(D) - P_m(D)\} \tag{28}$$

where $Q_{\Lambda_X^{(m)}}\{.\}$ denotes quantization to the closest point of the lattice $\Lambda_X^{(m)}$ underlying the power efficient modulo extension of the fundamental region of the mth signal constellation. We note that, by defining the signal $U_m(D) = A_m(D) + C_m(D)$ and observing the expression of $P_m(D)$, the signal $X_m(D)$ can be expressed as

$$X_m(D) = \frac{A_m(D) + C_m(D)}{1 + Dh^{(m)}(D)} = \frac{U_m(D)}{h_m(D)}. \tag{29}$$

Therefore, $U_m(D)$ represents the output of the mth subchannel in the absence of noise. To allow correct decoding operations with trellis coding performed across the subchannels, the symbol $U_m(nT)$ must represent a valid continuation of the code sequence $(\ldots, U_{m-2}(nT), U_{m-1}(nT))$, assuming the TCM state $\mathbf{y}_{m,n}$. Recalling that

- the mth signal constellation is a $N_m \times N_m$-point constellation with N_m even;
- $A_m(nT) \in \mathbf{B}_{y_{0,n}^{(m)}}$;
- $C_m(nT) \in \Lambda_X^{(m)}$;

we find that $U_m(nT) = A_m(nT) + C_m(nT) \in \mathbf{B}_{y_{0,n}^{(m)}}$. This implies that $U_m(nT)$ represents a valid continuation of the code sequence. To obtain a valid continuation of the code sequence also at the $(m+1)$th trellis precoding element, the information about the current TCM state $\mathbf{y}_{m,n}$ and about the chosen code symbol $U_m(nT)$ is sent to the $(m+1)$th next-state computation unit, which determines the state $\mathbf{y}_{m,n} = (y_{\nu-1,n}^{(m+1)}, \cdots, y_{0,n}^{(m+1)})$. After the $(M/2-1)$th trellis precoding element, a delay of one modulation interval is provided to allow the information about the TCM state and the chosen code symbol to be presented at

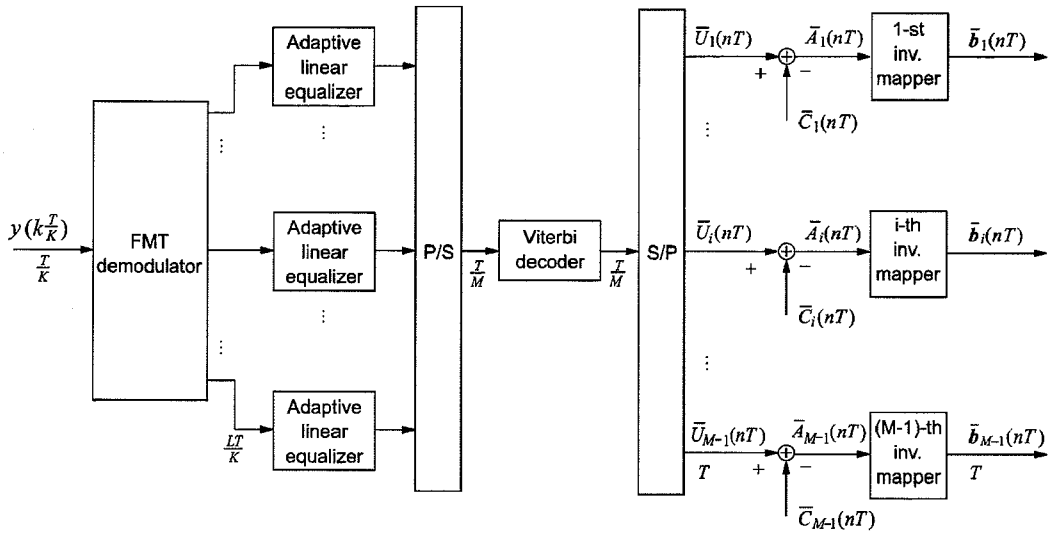

Fig. 10. FMT receiver with trellis-augmented precoding.

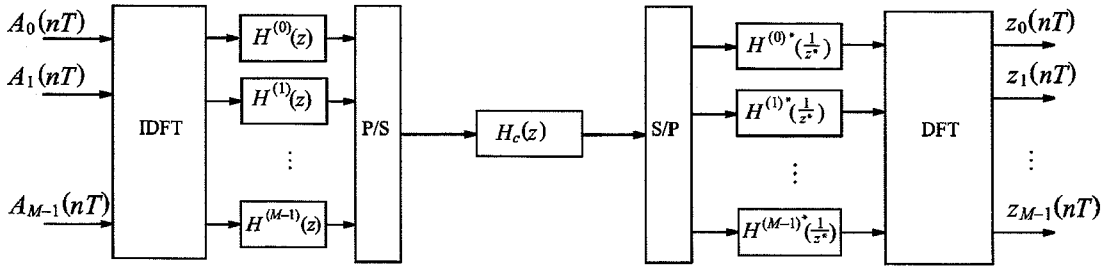

Fig. 11. Block diagram of a communication system with critically sampled filter banks ($K = M$).

the beginning of the next modulation interval at the input of the first element.

The block diagram of the receiver of an FMT system with trellis augmented precoding is illustrated in Fig. 10. The ith subchannel output signal is given by

$$V_m(D) = U_m(D) + W_m(D) \tag{30}$$

where $W_m(D)$ represents a sequence of additive Gaussian noise samples. In this receiver, per-subchannel linear adaptive equalization is included to compensate for mismatches between the subchannel frequency responses assumed at the transmitter and the actual responses. The M subchannel output signals are converted from parallel to serial, and the resulting sequence is input to the Viterbi decoder. The decoder output sequence $\hat{U}_m(D)$ is converted from serial to parallel. The detected sequences $\hat{A}_m(D)$, $m = 0, \ldots, M-1$, are then given by the memoryless operation

$$\hat{A}_m(D) = \hat{U}_m(D) - Q_{\Lambda_X^{(m)}}\{\hat{U}_m(D)\} = \hat{U}_m(D) - \hat{C}_m(D). \tag{31}$$

We note that error propagation in the receiver is completely avoided. The sequences of information vectors $\hat{\mathbf{b}}_m(D)$ are finally recovered from the sequences $\hat{A}_m(D)$.

Appendix B
Filter-Bank Design

To develop a prototype filter design algorithm for FMT, we determine the conditions for ICI suppression in a multicarrier system employing critically sampled uniform filter banks. For the special case of $K = M$, the modulator and demodulator structures derived in Section III take the simple form, first introduced in [11], depicted in Fig. 11. The prototype filter transfer functions at the transmitter and at the receiver are $H(z)$ and $H^*(1/z^*)$, respectively. Note that the commutators have been replaced by the equivalent parallel-to-serial (P/S) and serial-to-parallel (S/P) converters, and that the filtering elements on the M branches of the transmit and receive filter banks are not time-varying. Note also that the rate of the frames obtained at the DFT output is equal to the rate of the M input symbol sequences. We consider a normalized transmission interval $T/M = 1$. Let us express the transfer function of the prototype filter as

$$H(z) = \sum_{l=0}^{M-1} z^{-l} H^{(l)}(z^M) \tag{32}$$

where $H^{(l)}(z)$ denotes the transfer function of the lth polyphase component (with respect to M) of $H(z)$. We also express the transfer function of the noiseless channel in terms of its polyphase components as

$$H_c(z) = \sum_{l=0}^{M-1} z^{-l} H_c^{(l)}(z^M). \tag{33}$$

By repeatedly applying the noble identities [8, pp. 119–120], and the polyphase identity [8, p. 133], the transfer matrix of the filter bank communications system shown in Fig. 11 is expressed as

$$\Lambda(z) = \mathbf{F}\Gamma(z)\mathbf{F}^{-1} \tag{34}$$

where $\mathbf{F}$ and $\mathbf{F}^{-1}$ denote the DFT and IDFT matrices, respectively, and the matrix $\Gamma(z)$ is given by (35) shown at the bottom of the page.

Observing (34) and recalling that $\Lambda(z)$ is diagonal if and only if $\Gamma(z)$ is circulant, with elements on the diagonal given by the IDFT of the first row of $\Gamma(z)$, we find that a set of sufficient conditions for ICI suppression is given by

$$\begin{aligned}
&H^{(0)}(z)H^{(0)^*}\left(\frac{1}{z^*}\right)\\
&\quad = H^{(1)}(z)H^{(1)^*}\left(\frac{1}{z^*}\right) = \cdots\\
&\quad = H^{(M-1)}(z)H^{(M-1)^*}\left(\frac{1}{z^*}\right)\\
&H^{(1)}(z)H^{(0)^*}\left(\frac{1}{z^*}\right)\\
&\quad = H^{(2)}(z)H^{(1)^*}\left(\frac{1}{z^*}\right) = \cdots\\
&\quad = z^{-1}H^{(0)}(z)H^{(M-1)^*}\left(\frac{1}{z^*}\right)\\
&\cdots\\
&H^{(M-1)}(z)H^{(0)^*}\left(\frac{1}{z^*}\right)\\
&\quad = z^{-1}H^{(0)}(z)H^{(1)^*}\left(\frac{1}{z^*}\right) = \cdots\\
&\quad = z^{-1}H^{(M-2)}(z)H^{(M-1)^*}\left(\frac{1}{z^*}\right). \qquad (36)
\end{aligned}$$

Note that the conditions (36) cannot be satisfied in general by a FIR prototype filter, as they require strict band limitation within a subchannel. Furthermore, for an ideal channel with transfer function $H_c(z) = 1$, it can readily be seen that the conditions for ICI suppression are given by the first row of (36), which require that the correlation functions of the polyphase components are all equal. Therefore, if a linear phase FIR prototype filter is chosen that approximates a filter with strictly bandlimited frequency response and polyphase components that satisfy the first row of (36), then the system will exhibit no ICI if the channel is ideal and if the channel is nonideal the level of ICI will depend on the stopband attenuation. Let us define $H_{\text{ideal}}(z)$ as a filter that satisfies the equality

$$\begin{aligned}
&H_{\text{ideal}}(z)H^*_{\text{ideal}}(z)\left(\frac{1}{z^*}\right)\\
&\quad = H^{(0)}(z)H^{(0)^*}\left(\frac{1}{z^*}\right) = H^{(1)}(z)H^{(1)^*}\left(\frac{1}{z^*}\right) = \cdots\\
&\quad = H^{(M-1)}(z)H^{(M-1)^*}\left(\frac{1}{z^*}\right). \qquad (37)
\end{aligned}$$

Clearly, for an ideal transmission channel, (37) gives the transfer function of each subchannel. As mentioned in Section V, we consider FIR filters of length γM. Then each of the polyphase filter components has γ coefficients. The approximation problem is formulated first as an unconstrained optimization problem [21] and then is reduced to a form that requires finding the vector of filter coefficients

$$\begin{aligned}
&\Gamma(z)\\
&= \begin{bmatrix} H^{(0)}(z) & 0 & \cdots & 0\\ 0 & H^{(1)}(z) & \cdots & 0\\ \vdots & \vdots & \ddots & \vdots\\ 0 & 0 & \cdots & H^{(M-1)}(z)\end{bmatrix} \times \begin{bmatrix} z^{-1}H_c^{(0)}(z) & z^{-1}H_c^{(1)}(z) & \cdots & z^{-1}H_c^{(M-1)}(z)\\ z^{-2}H_c^{(M-1)}(z) & z^{-1}H^{(0)}(z) & \cdots & z^{-1}H_c^{(M-2)}(z)\\ \vdots & \vdots & \ddots & \vdots\\ z^{-2}H_c^{(1)}(z) & z^{-2}H_c^{(2)}(z) & \cdots & z^{-1}H_c^{(0)}(z)\end{bmatrix}\\
&\times \begin{bmatrix} \left(H^{(0)}\left(\frac{1}{z^*}\right)\right)^* & 0 & \cdots & 0\\ 0 & \left(H^{(1)}\left(\frac{1}{z^*}\right)\right)^* & \cdots & 0\\ \vdots & \vdots & \ddots & \vdots\\ 0 & 0 & \cdots & \left(H^{(M-1)}\left(\frac{1}{z^*}\right)\right)^*\end{bmatrix} = z^{-1}\\
&\times \begin{bmatrix} H^{(0)}(z)H_c^{(0)}(z)H^{(0)^*}\left(\frac{1}{z^*}\right) & H^{(1)}(z)H_c^{(1)}(z)H^{(0)^*}\left(\frac{1}{z^*}\right) & \cdots & H^{(M-1)}(z)H_c^{(M-1)}(z)H^{(0)^*}\left(\frac{1}{z^*}\right)\\ z^{-1}H^{(0)}(z)H_c^{(M-1)}(z)H^{(1)^*}\left(\frac{1}{z^*}\right) & H^{(1)}(z)H_c^{(0)}(z)H^{(1)^*}\left(\frac{1}{z^*}\right) & \cdots & H^{(M-1)}(z)H_c^{(M-2)}(z)H^{(1)^*}\left(\frac{1}{z^*}\right)\\ \vdots & \vdots & \ddots & \vdots\\ z^{-1}H^{(0)}(z)H_c^{(1)}(z)H^{(M-1)^*}\left(\frac{1}{z^*}\right) & z^{-1}H^{(1)}(z)H_c^{(2)}(z)H^{(M-1)^*}\left(\frac{1}{z^*}\right) & \cdots & H^{(M-1)}(z)H_c^{(0)}(z)H^{(M-1)^*}\left(\frac{1}{z^*}\right)\end{bmatrix}
\end{aligned}$$

(35)

$\mathbf{h} = [h(\gamma M/2), \ldots, h(\gamma M - 1)]$ that minimizes the quadratic objective function

$$\mathbf{h}^T\mathbf{S}^T\mathbf{S}\mathbf{h} + \frac{\kappa}{2}(\mathbf{J}\mathbf{h} - \boldsymbol{\nu})^T(\mathbf{J}\mathbf{h} - \boldsymbol{\nu}) \tag{38}$$

where the first term reflects the stopband mean energy of the prototype filter computed by dividing the stopband frequency interval $(\pi/M, M)$ in $N_s - 1$ subintervals, and the second term denotes the L_2 norm of the approximation error of condition (37). In (38), κ is a positive constant, and the elements of the matrices $\mathbf{S}$, $\mathbf{J}$, and the vector ν are given by

$$S(i, j) = \left[2\cos\left(\frac{2j+1}{2}(\omega_s + i\Delta\omega)\right)\right]$$
$$0 \le i \le N_s - 1 \quad 0 \le j \le \frac{\gamma M}{2} - 1$$

with $\omega_s = \pi/M$, $\Delta\omega = (\pi - \omega_s)/(N_s - 1)$

$$J(k + i\gamma, j) = \left[\tilde{J}\left(k + i\gamma, \frac{\gamma M}{2} + j\right) + \tilde{J}\left(k + i\gamma, \frac{\gamma M}{2} - 1 - j\right)\right]$$
$$0 \le k \le \gamma - 1, \quad 0 \le i \le M - 1$$
$$0 \le j \le \frac{\gamma M}{2} - 1$$

with

$$\tilde{J}(k + i\gamma, l) = \begin{cases} h(l - kM)\delta_{(l-i) \bmod M}, & \text{if } l \ge kM \\ 0, & \text{otherwise} \end{cases}$$
$$0 \le l \le \gamma M - 1$$

and $\nu(n) = (1/2\pi M)\int e^{j\omega[n \bmod \gamma]}|H_{\text{ideal}}(e^{j\omega})|^2\, d\omega$, $0 \le n \le \gamma M - 1$. The minimization of (38) can be performed, e.g., by an iterative least squares algorithm [22]. If the duration of the correlation function of $H_{\text{ideal}}(z)$ is greater than $2\gamma - 1$, windowing of the correlation may be used to avoid the Gibbs phenomenon. In general, large values of γ allow a better approximation of filters with transfer functions that exhibit sharp spectral roll-off and high attenuation of out-of-band energy, but lead to an increase in system latency. The choice of the prototype filter allows various tradeoffs between number of subchannels, level of spectral containment, signal latency, transmission efficiency, and complexity.

REFERENCES

[1] G. Cherubini, E. Eleftheriou, S. Ölçer, and J. Cioffi, "Frequency-division duplexing for VDSL," ITU-T, Study Group 15/4, Contribution NT-101, Nov. 1–5, 1999.

[2] F. Sjoberg, M. Isaksson, R. Nilsson, P. Ödling, S. K. Wilson, and P. O. Börjesson, "Zipper: A duplex method for VDSL based on DMT," *IEEE Trans. Commun.*, vol. 47, pp. 1245–1252, Aug. 1999.

[3] D. Mestdagh, M. Isaksson, and P. Ödling, "Zipper VDSL: A solution for robust duplex communication over telephone lines," *IEEE Commun. Mag.*, vol. 38, pp. 90–96, May 2000.

[4] G. Cherubini, E. Eleftheriou, and S. Ölçer, "Filtered multitone modulation for VDSL," in *Proc. IEEE Globecom'99*, Rio de Janeiro, Brazil, Dec. 1999, pp. 1139–1144.

[5] G. Cherubini, E. Eleftheriou, S. Ölçer, and J. Cioffi, "Filter bank modulation techniques for very high-speed digital subscriber lines," *IEEE Comm. Mag.*, vol. 38, pp. 98–104, May 2000.

[6] "Very-high-bit-rate digital subscriber line (VDSL) metallic interface. Part 1, 2 and 3," Committee T1, Working Group T1E1.4, Contribution T1E1.4/2000-009R3, -011, -013R4, Feb. 2001.

[7] N. Benvenuto, G. Cherubini, and L. Tomba, "Achievable bit rates of DMT and FMT systems in the presence of phase noise and multipath," in *Proc. IEEE Vehicular Technology Conf., VTC2000-Spring*, Tokyo, Japan, May 2000.

[8] P. P. Vaidyanathan, *Multirate Systems and Filter Banks*. Englewood Cliffs, NJ: Prentice-Hall, 1992.

[9] S. D. Sandberg and M. A. Tzannes, "Overlapped discrete multitone modulation for high speed copper wire communications," *IEEE J. Select. Areas Commun.*, vol. 13, pp. 1571–1585, Dec. 1995.

[10] F. Gardner, "Interpolation in digital modems: Part I: Fundamentals," *IEEE Trans. Commun.*, vol. 41, pp. 501–507, Mar. 1993.

[11] M. G. Bellanger, G. Bonnerot, and M. Coudreuse, "Digital filtering by polyphase network: Application to sample-rate alteration and filter banks," *IEEE Trans. Acoustics, Speech, Signal Processing*, vol. ASSP-24, pp. 109–114, Apr. 1976.

[12] K. Van Acker, G. Leus, M. Moonen, O. Van de Wiel, and T. Pollet, "Per tone equalization for DMT-based systems," *IEEE Trans. Commun.*, vol. 49, pp. 109–119, Jan. 2001.

[13] M. V. Eyuboglu and G. D. Forney, Jr., "Trellis precoding: Combined coding, precoding and shaping for intersymbol interference channels," *IEEE Trans. Inform. Theory*, vol. 38, pp. 301–314, Mar. 1992.

[14] R. Laroia, "Coding for intersymbol interference channels—Combined coding and precoding," *IEEE Trans. Inform. Theory*, vol. 42, pp. 1053–1061, July 1996.

[15] G. Cherubini, S. Ölçer, and G. Ungerboeck, "Trellis precoding for channels with spectral nulls," in *Proc. 1997 IEEE Int. Symp. Information Theory*, Ulm, Germany, June 29–July 4, 1997, p. 464.

[16] K. Mueller and M. Muller, "Timing recovery in digital synchronous data receivers," *IEEE Trans. Commun.*, vol. COM-24, pp. 516–531, May 1976.

[17] "Asymmetric digital subscriber line (ADSL) transceivers," ITU, Telecommunication Standardization Sector, Recommendation G.992.1, June 1999.

[18] G. Cherubini, E. Eleftheriou, S. Ölçer, J. Cioffi, and M. Sorbara, "Training of FMT transceivers," ITU-T, Study Group 15/4, Contribution FI-100, Jan. 31 Feb. 4, 2000.

[19] *Commercial Building Telecommunications Cabling Standard*, EIA-TIA Standard PN 2840, EIA/TIA 568-A, Mar. 1994.

[20] T. Starr, J. M. Cioffi, and P. J. Silverman, *Digital Subscriber Line Technology*. Englewood Cliffs, NJ: Prentice-Hall, 1999.

[21] J. Princen, "The design of nonuniform modulated filter banks," *IEEE Trans. Signal Processing*, vol. 43, pp. 2550–2560, Nov. 1995.

[22] M. Rossi, J.-Y. Zhang, and W. Steenaart, "Iterative least squares design of perfect reconstruction QMF banks," in *Proc. IEEE CCECE'96*, 1996, pp. 762–765.

[23] G. Cherubini, E. Eleftheriou, S. Ölçer, and J. Cioffi, "Frequency-division duplexing for VDSL," Committee T1, Study Group T1E1.4, Contribution T1E1.4/99-556, Dec. 6, 1999.

[24] G. Cherubini, E. Eleftheriou, S. Ölçer, J. Cioffi, and M. Sorbara, "Training of FMT transceivers," Committee T1, Study Group T1E1.4, Contribution T1E1.4/2000-072, Feb. 21, 2000.

Giovanni Cherubini (S'80–M'82–SM'94) received the Dr.Ing. degree in electrical engineering, (*summa cum laude*), from the University of Padova, Padova, Italy, in 1981, and the M.S. and Ph.D. degrees in electrical engineering from the University of California, San Diego, in 1984 and 1986, respectively. In 1984, he received a scholarship from M/A-COM Linkabit, San Diego, CA, for his work on the synchronization of spread-spectrum systems.

Since 1987, he has been with the IBM Zurich Research Laboratory, Rüschlikon, Switzerland. His research interests include the study of transceiver architectures for high-speed data transmission and signal processing for bandwidth-efficient communications.

Dr. Cherubini served as Guest Editor for the Special Issues of the IEEE JOURNAL ON SELECTED AREAS IN COMMUNICATIONS on Copper Wire Access Technologies for High-Performance Networks, and on Multiuser Detection Techniques with Application to Wired and Wireless Communications Systems. From 1995 to 1996, he was coeditor of the IEEE Standard 100BASE-T2 for Fast Ethernet transmission over voice-grade cables. Since 1999, he has been Editor for CDMA Systems for the IEEE TRANSACTIONS ON COMMUNICATIONS.

Evangelos Eleftheriou (SM'00–F'02) received the B.S. degree in electrical engineering from the University of Patras, Patras, Greece, in 1979, and the M.Eng. and Ph.D. degrees in electrical engineering from Carleton University, Ottawa, Canada, in 1981 and 1985, respectively.

He joined the IBM Zurich Research Laboratory in Rüschlikon, Switzerland, in 1986, where he has been working in the areas of high-speed voice-band data modems, wireless communications, and coding and signal processing for the magnetic recording channel. Since 1998, he has managed the magnetic recording and wired transmission activities at the IBM Zurich Research Laboratory. His primary research interests lie in the areas of communications and information theory, particularly signal processing and coding for recording and transmission systems. He holds over 30 patents (granted and pending applications) in the areas of coding and detection for transmission and digital recording systems, and was named a Master Inventor at IBM Research, in 1999.

Dr. Eleftheriou was Editor of the IEEE TRANSACTIONS ON COMMUNICATIONS from 1994 to 1999 in the area of equalization and coding. He was Guest Editor for the Special Issue of the IEEE JOURNAL ON SELECTED AREAS IN COMMUNICATIONS on The Turbo Principle: From Theory to Practice.

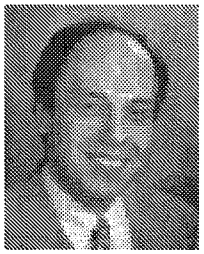

Sedat Ölçer (SM'94) received the Diploma of electrical engineering and the Ph.D. degree from the Swiss Federal Institute of Technology, Lausanne (EPFL), Switzerland, in 1978 and 1982, respectively.

From 1982 to 1984, he was a Research Associate at the Information Systems Laboratory of Stanford University, Stanford, CA, and at Yale University, New Haven, CT.

In 1984, he joined the IBM Zurich Research Laboratory, Rüschlikon, Switzerland, where he worked on digital transmission techniques for magnetic recording channels and, more recently, on high-speed data communications for local area networking and network access. His research interests are in digital communications, signal processing and coding, with applications to broadband network access. In 1999, Dr. Ölçer was Guest Editor for the special issue of *Computer Networks* on Broadband Access Networks, and in 2000, he served as Guest Editor of the *IEEE Communication Magazine* Feature Topic on Very High-Speed Digital Subscriber Lines. He is currently a Technical Editor of the *IEEE Communications Magazine*.